MALAYSIAN JOURNAL OF SCIENCE
MJS
ISSN 1394-3065

Regular Issue

Malaysian Journal of Science 44 (1): 1-8 (March 2025) https://mjs.um.edu.my

Lignin and Cellulose Nanofibers from *Bambusa vulgaris* Schrad (Bamboo): An Extraction, Preparation and Characterization Study

Tawakaltu AbdulRasheed-Adeleke[1a], Evans Chidi Egwim[2a], Stephen Shaibu Ochigbo[3b], Adefowope Saheed Alabi[4c], Christopher Chintua Enweremadu[5d] and Joshua Olusegun Okeniyi[6de]*

Abstract: In this paper, lignin and cellulose nanofibers were extracted and prepared from *Bambusa vulgaris* schrad (*B. vulgaris*: bamboo) before being subjected to characterization investigations. These extractions and preparations of the lignin and cellulose nanofibers were carried out chemically using alkali combined with bleaching treatments together with acid hydrolysis and sonication. The cellulose nanofibers were then subjected to morphological and dimensional characterization of the Zetasizer, Scanning Electron Microscopy (SEM) and Transmission Electron Microscopy (TEM) instruments. The functional groups investigation, using Fourier Transform infrared spectroscopy (FTIR), and thermal degradation via the Thermogravimetric analysis (TGA), of the bamboo lignin and of the cellulose nanofibers were also carried out. Results revealed that the percentage yields of the bamboo lignin and bamboo nanofiber were 21.91 wt% and 33.6 wt% respectively. The SEM and TEM investigations indicated the prepared nanofibers were rod-like in morphology, having sizes ranging from 20 to 100 nm. FTIR showed that the lignin extracted from bamboo typified G-S type lignin while the nanofibers are completely devoid of lignin. TGA revealed that the lignin was more thermally stable than the nanofiber under the test conditions. The obtained lignin and cellulose nanofibers showed promise for possible application as reinforcement agents in biodegradable nanocomposite film preparation.

Keywords: *Bamboo, cellulose nanofibers, lignin, materials extraction, materials characterization.*

1. Introduction

Cellulose and lignin are natural organic polymers found mainly in plants. Cellulose is the most widely available biopolymer having straight chain of D-glucose units, which are linked together via the bonds of $\beta(1 \rightarrow 4)$-glycosides (Vazquez et al., 2013). It is a fundamental structural constituent of plants' primary cell wall, and of some species of algae, as well as of the oomycetes. It is also known that some species of bacteria also secrete cellulose for the formation of biofilms (Brethauer et al., 2020; Beloin et al., 2008). In contrast, lignin is a polymeric natural product resulting from trans-coniferyl alcohol, trans-sinapyl alcohol and trans p-coumaryl alcohol polymerization (Harman-Ware et al., 2017). Lignin is a complicated compound that is generally obtained from wood, while it is also a plants' secondary cell walls fundamental component, and that is also present in some algae (Börcsök et al., 2020; Labeeuw et al., 2015; Lebo, et al., 2015; Martone, et al., 2009). Since lignin and hemicellulose are covalently linked, lignin crosslinks diverse polysaccharides of plants, and by this, gives mechanical strength to the plant's cell wall, which extend as structural strength to the whole plant actually (Jawerth et al., 2020; Salmén et al., 2016; Gibson 2012; Chabannes et al., 2001).

Cellulose and lignin have been extracted from many plants using several methods that have been reported by many authors (Dinh Vu et al., 2017; Radotić & Mićić 2016; Yong et al., 2012; Kaushik et al., 2010; Alemdar & Sain, 2008). These extractions, of both cellulose and lignin, have been put into many applications, several of which have also been detailed in the literature (Gopakumar et al., 2018; Atanda, 2015; Zakikhani et al., 2014; Bao et al., 2011). For instance, fibers obtained from these extractions can be in micro or nano form. Currently, the nano form is favored owing to the exceptional effect such as the outstanding mechanical properties that could be obtained from only a little content of the nanofiller. A variety of methods have also been employed for preparing and extracting nanofibers of high purity from cellulosic materials (Shahi et al., 2020; Phanthong et al., 2018; Menon et al., 2017; Xiao et al., 2015; Lu et al., 2013; Saito et al., 2009; Paakko et al., 2007; Elazzouzi-Hafraoui et al., 2008; Alemdar & Sain 2008).

Bambusa vulgaris schrad (*B. vulgaris*: bamboo) is a naturally occurring biomass, which grows plentifully in most of the sub-tropical countries. Also, that *B. vulgaris* contains cellulose fibers imbedded in a lignin matrix makes it to be regarded as a

Authors information:
[a]Department of Biochemistry, Federal University of Technology, Minna, Niger State, NIGERIA. Email: tawarash@yahoo.com[1], c.egwim@futminna.edu.ng[2]
[b]Department of Chemistry, Federal University of Technology, Minna, Niger State, NIGERIA. E-mail: stephenochigbo@futminna.edu.ng[3]
[c]School of Business, Project Management Department, St Lawrence College, Kingston, Ontario, CANADA. E-mail: adefowope.alabi@sl.on.ca[4]
[d]Department of Mechanical, Bioresources and Biomedical Engineering, University of South Africa, Pretoria, SOUTH AFRICA. E-mail: enwercc@unisa.ac.za[5], joshua.okeniyi@covenantuniversity.edu.ng[6]
[e]Department of Mechanical Engineering, Covenant University, Ota, Ogun State, NIGERIA. E-mail: joshua.okeniyi@covenantuniversity.edu.ng[6]
Corresponding Author: joshua.okeniyi@covenantuniversity.edu.ng

Received: January 24, 2023
Accepted: July 5, 2023
Published: March 31, 2025

DOI: https//doi.org/10.22452/mjs.vol44no1.1
Malaysian Journal of Science 43(4): 1-8 (March 2025)

composite material. This composite material exhibits many advantages, which among others includes strength, durability, light weight, stiffness, and biodegradability, and by these, *B. vulgaris* has found applications, from time memorial, in many sectors (Rahim et al., 2018; Atanda, 2015; Zakikhani et al., 2014; Atanda, 2015; Bao et al., 2011). Although *B. vulgaris* (bamboo) is readily available in Nigeria, it is highly underutilized (Atanda, 2015), and it has not been extensively studied as a source of nanofibers (Saniwan, et al., 2012; John et al., 2007; Chakraborty et al., 2006). Hence, the focus of this study is on the application of bamboo for preparing and characterizing nanofibers and lignin.

2. Materials and Methods

Materials

Sample materials and chemicals

Collections of the stems of *B. vulgaris* (bamboo) were from the banks of River Gurara at Izom, Niger State, Nigeria. These *B. vulgaris* stems were identified and authenticated at the herbarium of National Institute for Pharmaceutical Research and Development (NIPRD), Idu, Abuja, Nigeria, where a voucher of No NIPRD/H/6793 had been dropped for future reference. Purchased from reputable chemical stores for the study include analytical grades of C_2H_5COH, H_2SO_4 and H_2O_2 (from BDH Chemicals®, England), NaOH (from Kermel®, China), and HCl (from Griffin and George®, England).

Equipment

The equipment employed in this study are: Oven (Gallenkamp® Size 2, 11526E), Autoclave (Patterson Scientific®, Prestige 2100), Digital Weighing Balance (Ohaus Cooperation®, China, Scout Pro SPU601), pH meter (Hanna®, pH 212), Thermogravimetric analyzer (Perkin Elmer® STA 6000), Transmission Electron Microscope (Zeiss Auriga® HRTEM), Scanning Electron Microscope (Zeiss Auriga® HRSEM), Fourier Transform Infrared (Perkin Elmer®, UK, Frontier FT-IR), Ultra Sonicator (Scientz®, China, SB25-12DT), Zetasizer (Malven®, USA, Nano-S series).

B. vulgaris Fiber and Lignin Preparation

The extraction of lignin from *B. vulgaris* followed the method that had been detailed in the research works reported by Yong et al. (2012), Kaushik et al. (2010) and Alemdar & Sain (2008). By these, stalks of *B. vulgaris* were sun-dried before being chopped to smaller pieces. This was followed by grinding the chopped pieces and subsequent screening to a mesh fraction of 40–60 µm. From this ground stalk of *B. vulgaris*, 20 g was soaked in 4% w/w NaOH, for 24 h at room temperature, after which it was filtered and washed with distilled water until the complete elimination of the alkali. Further filtration was carried out for the second time before treatment with 10% w/w NaOH for 4 h in an autoclave maintained at 121 °C. Rewashing of the material with distilled water and subsequent filtration then followed. The filtrate was then acidified with H_2SO_4 to pH = 2 for the precipitation of lignin. The precipitated lignin were then filtered out of the mixture, separated and was then washed severally with water before being dried in an oven set at 40 °C. The supernatant ensuing from the alkali treatment was bleached, at room temperature, in 8 % v/v H_2O_2 for 24 h to obtain *B. vulgaris* fiber, which was washed and filtered over and over again, just like before, for obtaining the fiber material from the plant, for further use.

Preparation of Nanofiber from *B. vulgaris* Fiber

Preparation of nanofiber from *B. vulgaris* fibers was done through acid hydrolysis usage (Saniwan et al., 2012 Kaushik et al., 2010). The *B. vulgaris* fibers were steeped in 10 %w/w HCl with applied ultrasonic agitation, by an ultrasonicator (SB25-12DT, Scientz®, China), for 2 h and at 60 °C. Final washing of the sample material then followed, before the homogenization of the same for 15 min in a Heidolph® DIAX 900 (USA) high shear homogenizer instrument for obtaining *B. vulgaris* nanofibers.

B. vulgaris Nanofiber and *B. vulgaris* Lignin Characterizations

Percentage yield analyses

The determinations of *B. vulgaris* nanofiber and *B. vulgaris* lignin yields were obtained from the dry weight of the sample material that was isolated based on the initial dry weight of grinded *B. vulgaris*.

Nanofiber Particle Size Analyses

Investigation of *B. vulgaris* nanofiber particle sizes in solution employed use of dynamic light scattering (DLS) by the Zetasizer Nano-S series instrument from Malven®, USA, at 173° angle of light scattering, 25°C operating temperature, and 120 sec equilibrating time. For carrying out the particle size analysis, 1 mg of the sample material was dispersed in 10 ml C_2H_5OH before being transferred, using a syringe having 0.22 µm filter coupled to it, into a polystyrene cuvette. This was then placed into in the analysis stage of the Zetasizer equipment for analyzing the *B. vulgaris* nanofiber particle sizes.

Spectra Analyses

Spectra analyses of the *B. vulgaris* nanofiber and *B. vulgaris* lignin were carried out using the Frontier FT-IR, Perkin Elma® (UK) machine, by KBr disc, with spectra range between 4000 and 400 cm^{-1}. This was used for assessing the changes in the chemical structure of the polymer, which could have taken place due to modification.

Thermal Behavior Analyses

The *B. vulgaris* nanofiber and *B. vulgaris* lignin thermal behaviors were studied using the STA 6000 model of Thermogravimetric analyzer (from Perkin Elmer®).

Morphological Analyses

Morphological investigations of the *B. vulgaris* nanofiber were done via use of the HRSEM model of Scanning Electron Microscopy (SEM) instrument (from Zeiss Auriga®) at a voltage of 15 kV. The samples for the SEM analyses were mounted on the stub having two-sided adhesive tape having a thin layer of gold for its coating (Okeniyi et al., 2018; Okeniyi et al., 2017a; Okeniyi et al., 2017b), for the non-conducting *B. vulgaris* nanofibers being

DOI: https//doi.org/10.22452/mjs.vol44no1.1
Malaysian Journal of Science 43(4): 1-8 (March 2025)

investigated. A 350 times the original size were then used as the magnification for taking the images by the SEM equipment, as detailed in Kampeerapappun et al. (2007).

Transmission Electron Microscopy (TEM)

High resolution Transmission electron microscopy (HRTEM) measurements employed the use of the Zeiss Auriga® HRTEM instrument at 100kV. Samples of *B. vulgaris* nanofiber were diluted in distilled water at the ratio of 1 part *B. vulgaris* nanofiber to 20 parts distilled water. Copper grids, at 300-mesh grid sizes, were then dipped in the diluted *B. vulgaris* nanofiber solutions before the grids are dried at ambient temperature. The TEM images of the *B. vulgaris* nanofiber samples were then taken with the microscope. For these, high magnifications at 30,000 and 85,000 times the original sample size were then employed for taking images of the *B. vulgaris* nanofiber samples (Ochigbo et al., 2012; Kampeerapappun et al., 2007).

4. Discussion

Percentage Yields of *B. vulgaris* Nanofiber and Lignin

The images of *B. vulgaris* nanofiber and *B. vulgaris* lignin are presented in Figure 1. The respective percentage yields of these materials are 33.6% and 21.91%, respectively.

Figure 1. Post-processing images of (a) *B. vulgaris* lignin, and (b) *B. vulgaris* nanofiber.

***B. vulgaris* Nanofiber Size Distribution**

The particle size distribution, of the *B. vulgaris* nanofiber sample studied, is presented in Figure 2.

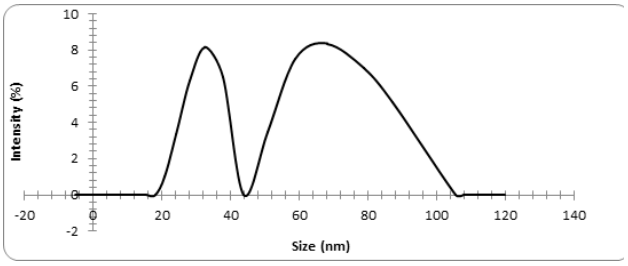

Figure 2. *B. vulgaris* nanofiber particle size distribution.

From Figure 2, the particle size distribution showed that *B. vulgaris* nanofiber had two granulometric distributions with the peak of the first at 30 nm, while the peak of the second is at 70 nm. Also, it could be observed that range of the prepared nanofiber sizes is from 20 nm to 100 nm, which indicates the fibers prepared in the present study are in the nano-sized scale. By this, therefore, the fibers could be suitable for use as fillers in the production of nanocomposite films.

Micrographs of the Prepared *B. vulgaris* Nanofiber

The micrographs, obtained from the SEM and TEM instruments, of the prepared *B. vulgaris* nanofiber, are shown in Figure 3. From Figure 3a, the SEM depicted the prepared *B. vulgaris* nanofibers as rod-like, whereas the micrograph from the TEM instrument, Figure 3b, indicated the prepared nanofibers ranged from 20 nm to 100 nm in size. These results from the TEM equipment confirm the *B. vulgaris* particle size distribution from Figure 2 that had been obtained using another instrument, i.e. the Zetasizer Nano-S series. From Figure 3b, it could also be deduced that the amorphous regions of the nanofiber were transversely cleaved by exposure to hydrochloric acid hydrolysis, thereby reducing the fibers sizes from microns to nanometers (Yong et al., 2012; Azazi-Samir et al., 2005). The result obtained herein exhibited agreement that from Liu et al. (2010), from which the size ranging between 50 nm and 100 nm cellulose nanocrystals were produced from the treatment of strands from bamboo by HNO_3-$KClO_3$ that was followed by acid hydrolysis. In another related study, Krishnan & Ramesh (2013) also reported particle width range from 30 nm to 90 nm for nanofibers obtained from coconut coir fibers, which is just as Zhang et al. (2007) obtained spherically shaped cellulose nanoparticle materials. The difference in shape of the various nanofibers obtained could be ascribed to the type of treatment used. By the morphological results in the present case, the *B. vulgaris* nanofibers, so prepared, are found appropriate as fillers in the productions of starch nanocomposite films.

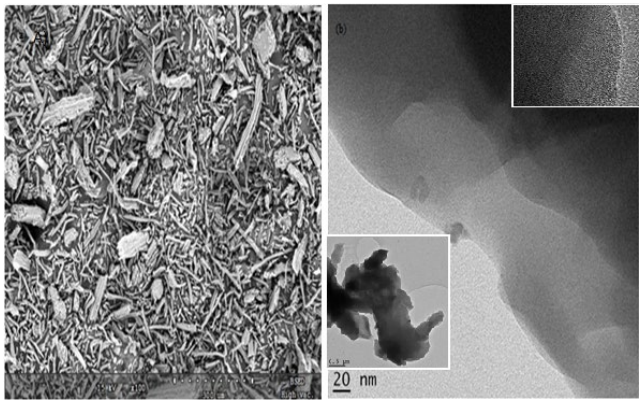

Figure 3. Micrographs of the prepared *B. vulgaris* nanofiber (a) SEM (b) TEM.

FTIR Spectra of *B. vulgaris* Lignin and *B. vulgaris* Nanofiber

The FTIR spectra from the *B. vulgaris* lignin and the *B. vulgaris* nanofiber are presented in Figure 4. The functional groups distribution proposed for assignments at adsorbed frequencies resulting from the FTIR spectra are presented in Table 1 (Okeniyi et al., 2019; Okeniyi & Popoola, 2017; Okeniyi et al., 2017c; Okeniyi et al., 2016; Coates, 2000).

DOI: https//doi.org/10.22452/mjs.vol44no1.1
Malaysian Journal of Science 43(4): 1-8 (March 2025)

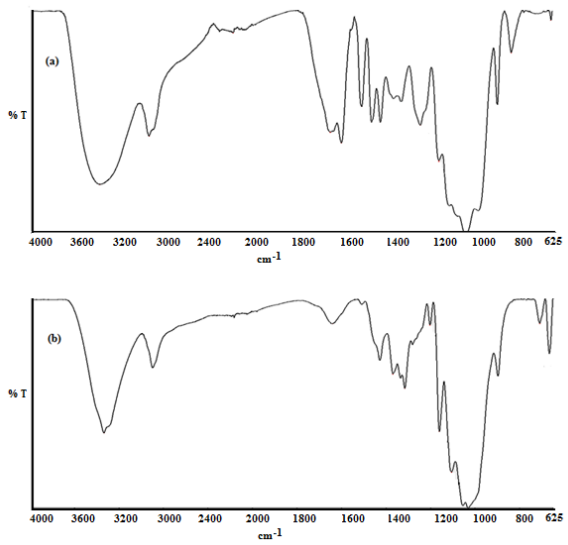

Figure 4. FTIR Spectra of (a) *B. vulgaris* lignin and (b) *B. vulgaris* nanofiber.

Table 1. Assignments of FTIR Spectra Frequencies from *B. vulgaris* lignin and *B. vulgaris* nanofiber.

***B. vulgaris* Lignin Frequency (cm^{-1})**	***B. vulgaris* Nanofiber Frequency (cm^{-1})**	**Chemical Groups Assignment**
3364	3335	aliphatic and aromatic O–H stretch
2922, 2167	2899	saturated aliphatic C–H stretch
1648	1639	carbonyl stretch (conjugated ketone)
1597, 1506, 1461	-	Aromatic C=C–C rings stretching and bending vibrations
1422	1428	C–H in-plane bend deformation
-	1368	O–H bend induced by groups of phenol
1328	1316	C–O breathing of Syringyl ring
1242	-	C–O breathing of Guaiacyl ring
1159	1160, 1105	C–O stretch vibration of alkyl/cyclic ethers
896, 834	897	C–H ring deformation from di-substituted aryl groups
-	709, 666	O–H out-of-plane bending vibration

From the presented results in Table 1, the following characteristic absorption bands derived from the FTIR spectrum of *B. vulgaris* lignin include the absorption band at 3364 cm^{-1} that is attributed to the stretching vibration of O–H in aliphatic OH and aromatic groups, while the bands in the proximities of 2922 cm^{-1} and of 2167 cm^{-1} respectively corresponds to saturated aliphatic CH_2's asymmetrical and symmetrical stretching bands. The 1648 cm^{-1} absorption band is allocated to the stretching of conjugated carbonyl groups. Absorption bands at 1422 cm^{-1}, 1506 cm^{-1} and 1597 cm^{-1} are attributed to the skeleton vibration of aromatic groups in the *B. vulgaris* lignin. The 1461 cm^{-1} absorption frequency illustrates aromatic ring vibration and C–H deformations, while the adsorption at 1242 cm^{-1} frequency follows from guaiacyl (G) ring breathing with C–O.

In the *B. vulgaris* nanofiber, the 1368 cm^{-1} absorption frequency corresponds to O–H groups of free phenolic compounds. The absorptions at 1316 cm^{-1} from the *B. vulgaris* nanofiber spectra and at 1328 cm^{-1} by the *B. vulgaris* lignin spectra indicate syringyl (S) ring breathing with C-O. The adsorbed frequencies at 896 cm^{-1} and 1159 cm^{-1} are respectively attributed to C–O deformation and ether stretching. Finally, the adsorption at 834 cm^{-1} corresponds to ring vibrations and C–H deformation.

The distributions of functional groups for *B. vulgaris* lignin, in this study, conform to the result reported in literature for Kraft and Klason lignin extracted from pine and wood (Faix, 1991; Zheng-Jun et al., 2012b; Ghatak, 2008; Li, 2011; Ibrahim et al., 2006). In more specific terms, in the system of lignin infrared spectra classified by Faix (1991), the extracted *B. vulgaris* lignin was typically of the G-S type of lignin owing to the consideration that the absorption at 1463 cm^{-1} is of a lower intensity than the band at 1508 cm^{-1}, in that study. Also, the peak of absorption frequency obtained in that study at 1248 cm^{-1} is of a stronger intensity than the peak that was obtained at 1325 cm^{-1}, by Faix (1991).

The spectrum of FTIR obtained from *B. vulgaris* nanofiber compares well with that of *B. vulgaris* lignin, with the contrast that the absorption bands at 1506 cm^{-1} and 1597 cm^{-1}, which correspond to aryl ring of C=C–C stretching from the lignin, are absent. The non-availability of these peaks in *B. vulgaris* nanofiber is attributed to lignin elimination as a result of further acid hydrolysis in *B. vulgaris* nanofiber preparation process. Also, the peak at 1242 cm^{-1} is also absent in the *B. vulgaris* nanofiber, which illustrates the effective elimination of hemicelluloses, lignin and pectin in the process of the *B. vulgaris* nanofiber preparation.

Thermal Behaviors of *B. vulgaris* Lignin and *B. vulgaris* Nanofiber

Presented in Figure 5 are the thermal behaviors of *B. vulgaris* lignin and *B. vulgaris* nanofiber, while the essential parameters of degradation data from the thermal characterizations are plotted in Figure 6.

DOI: https//doi.org/10.22452/mjs.vol44no1.1
Malaysian Journal of Science 43(4): 1-8 (March 2025)

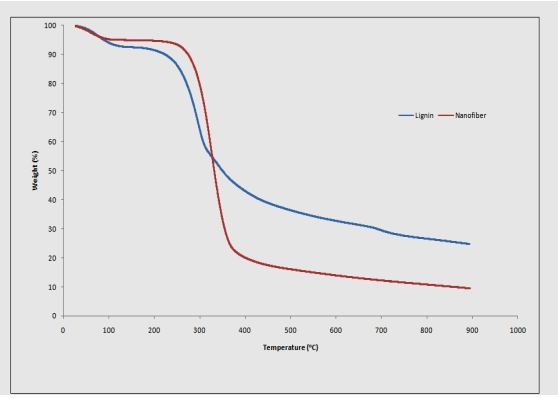

(a)

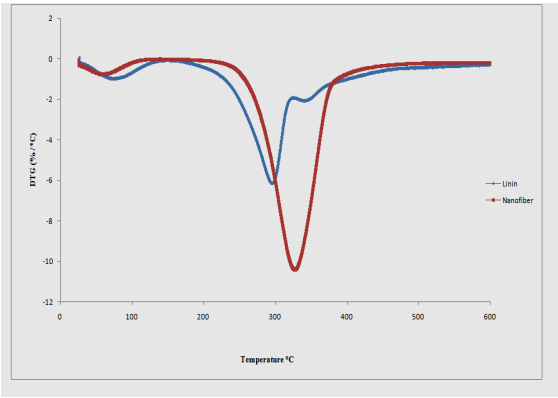

(b)

Figure 5. TGA thermograms: (a) *B. vulgaris* lignin; (b) *B. vulgaris* nanofiber.

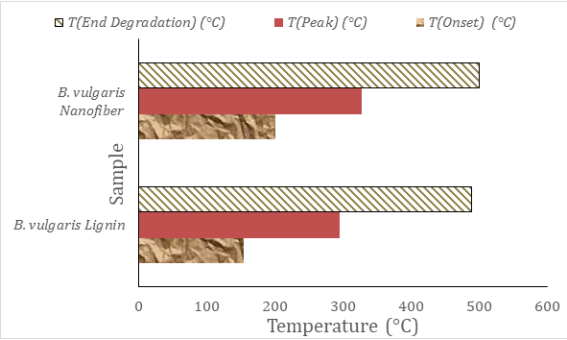

(a)

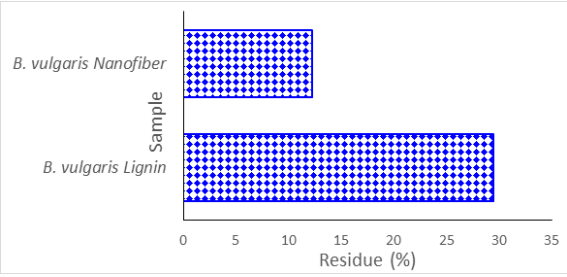

(b)

Figure 6. Plots of TGA degradation parameters from *B. vulgaris* lignin and *B. vulgaris* nanofiber thermal behavior (a) Temperature data (b) post TGA residue.

From Figure 5, it could be noted that three degradation stages occurred in lignin. The evolution of moisture content of the lignin sample was indicated by the initial weight loss that occurred at the temperature of about 96 °C. The evolution of products that are of low molecular weight such as CO_2, CO and CH_4 occurred at 154 °C and this is termed onset degradation (Visakh et al., 2012a; LeVan, 1989). The peak degradation and end degradation occurred at 295 °C and 488 °C respectively with solid residue of about 29.45%. At temperatures above 500 °C, denoting the third stage, weight loss was no more obvious due to the condensation reactions of aromatic rings that often occur concurrently with decomposition reactions, at this stage, (Zheng-Jun et al., 2012; Visakh et al., 2012a; LeVan, 1989). These observed thermal behaviors by *B. vulgaris* lignin in the present study exhibit similarity with that obtained from reported research works, carried out on other biological materials, by other authors including Shi et al. (2012), Sumin et al. (2012), and Li (2011).

Alternatively, the TGA plotting of the *B. vulgaris* nanofiber sample occurred in two degradation stages, during the pyrolytic degradation process. From this, an onset degradation temperature occurred at around 200 °C, which was higher than the onset degradation temperature of lignin. In the 2nd degradation stage, a sharp decomposition was observed with the peak temperature of decomposition and of end degradation occurring at 328 °C and 500 °C, respectively. Severe weight loss also occurred such that only about 12.2% remained from the initial sample of *B. vulgaris* nanofiber. The lower percentage of residue that was observed in the *B. vulgaris* nanofiber, in comparison to that of the *B. vulgaris* lignin, could be ascribed to the non-availability of mineral substances, generally oxides, in the *B. vulgaris* nanofiber. The thermogravimetric degradation behavior, detailed in the present work from *B. vulgaris* nanofiber, exhibits similarity to results obtained by Visakh et al. (2012b) and LeVan (1989).

Based on the foregoing consideration, it could be inferred that *B. vulgaris* lignin exhibits more thermal stability than the *B. vulgaris* nanofiber, under the condition at which the measurements in the study were carried out. This is in spite of the fact that the degradation occurring from *B. vulgaris* lignin began at lower temperature than the degradation from the *B. vulgaris* nanofiber.

5. Conclusion

Lignin and nanofibers were successfully extracted and prepared from *B. vulgaris* (bamboo). The morphology of the prepared *B. vulgaris* nanofibers were revealed, by SEM and TEM analyses, to be rod-shaped having sizes that range from 20 to 100 nm. FTIR showed that the lignin extracted from *B. vulgaris* is G-S lignin type while the *B. vulgaris* nanofibers are mostly devoid of lignin. TGA showed that the *B. vulgaris* lignin was more thermally stable than that of the *B. vulgaris* nanofiber under the condition that they were measured.

DOI: https//doi.org/10.22452/mjs.vol44no1.1
Malaysian Journal of Science 43(4): 1-8 (March 2025)

6. References

Atanda, J. (2015). Environmental impacts of bamboo as a substitute constructional material in Nigeria. *Case Studies in Construction Materials* 3:33–39.

Alemdar, A., Sain, M. (2008). Isolation and characterization of nanofibers from agricultural residues, Wheat straw and soy hulls. *Bioresource Technology,* 99:1664–1671.

Azizi-Samir, M.A.S., Alloin, F., Dufresne, A. (2005). Review of recent research into cellulosic whiskers, their properties and their application in nanocomposite field. *Biomacromolecules*, 6:612–626.

Bao, L., Chen, Y., Zhou, W., Wu, Y., Huang, Y. (2011). Bamboo fibers at poly(ethylene glycol) reinforced poly (butylenes succinate) biocomposites. *Journal of Applied Polymer Science,* 122:2456–2466.

Beloin C., Roux A., Ghigo J.-M. (2008). "*Escherichia coli* Biofilms." In: Romeo, T. (ed.) *Bacterial biofilms. Current Topics in Microbiology and Immunology (Volume 322)*. Springer-Verlag Berlin Heidelberg, 249–289.

Brethauer, S., Shahab, R.L., Studer, M.H. (2020). Impacts of biofilms on the conversion of cellulose. *Applied Microbiology and Biotechnology*, 104:5201–5212.

Börcsök, Z., Pásztory, Z. (2020). The role of lignin in wood working processes using elevated temperatures: an abbreviated literature survey. *European Journal of Wood and Wood Products*, doi:10.1007/s00107-020-01637-3.

Chabannes, M., Ruel, K., Yoshinaga, A., Chabbert, B., Jauneau, A., Joseleau, J.P., Boudet, A.M. (2001). *In situ* analysis of lignins in transgenic tobacco reveals a differential impact of individual transformations on the spatial patterns of lignin deposition at the cellular and subcellular levels. *Plant Journal,* 28(3):271–282

Chakraborty, A., Sain, M., Kortschot, M. (2006). Reinforcing potential of wood pulp-derived microfibers in a PVA matrix. *Holzforschung*, 60:53–8.

Coates, J. (2000). "Interpretation of infrared spectra, a practical approach." In: Meyers, R.A. (Ed.), *Encyclopedia of Analytical Chemistry*, 10815-10837.

Dinh Vu, N., Thi Tran, H., Bui, N.D., Duc Vu, C., Viet Nguyen, H. (2017). Lignin and cellulose extraction from Vietnam's rice straw using ultrasound-assisted alkaline treatment method. *International Journal of Polymer Science*, 2017:1063695.

Elazzouzi-Hafraoui, S., Nishiyama, Y., Putaux, J.L., Heux, L., Dubreuil, F., Rochas, C. (2008). The shape and size distribution of crystalline nanoparticles prepared by acid hydrolysis of native cellulose. *Biomacromolecules*, 9 (1):57–65.

Faix, O. (1991). Classification of lignins from different botanical origins by FT-IR spectroscopy. *Holzforschung,* 45:21–27.

Ghatak, H.R. (2008). Spectroscopic comparison of lignin separated by electrolysis and acid precipitation of wheat straw soda black liquor. *Industrial Crops and Products,* 28(2):206–212.

Gibson, L.J. (2012). The hierarchical structure and mechanics of plant materials. *Journal of the Royal Society Interface*, 9(76):2749–2766.

Gopakumar, D.A., Manna, S., Pasquini, D., Thomas, S. and Grohens, Y. (2018). Nanocellulose: extraction and application as a sustainable material for wastewater purification. In: Hussain, C.M. and Mishra, A.K. (Eds.) *New Polymer Nanocomposites for Environmental Remediation,* Elsevier Inc., 469–486.

Harman-Ware, A.E., Happs, R.M., Davison, B.H. and Davis, M.F. (2017). The effect of coumaryl alcohol incorporation on the structure and composition of lignin dehydrogenation polymers. *Biotechnology for Biofuels*, 10(1):1–11.

Ibrahim, M.N., Mohamad, A.H., Yusop M.R.M. (2006). The effects of lignin purification on the performance of iron complex drilling mud thinner. *Jurnal Teknologi*. 44:83–94.

Jawerth, M.E., Brett, C.J., Terrier, C., Larsson, P.T., Lawoko, M., Roth, S.V., Lundmark, S., Johansson, M. (2020). Mechanical and morphological properties of lignin-based thermosets. *ACS Applied Polymer Materials*, 2(2):668–676.

John, M.J., Anandjiwala, R.D., Pothan, L.A., Thomas, S. (2007). Cellulosic fiber reinforced green composites. *Composite Interface*, 14 (7–9):733–751.

Kampeerapappun, P., Aht-ong, D., Pentrakoon, D. and Srikulkit, K., 2007. Preparation of cassava starch/montmorillonite composite film. *Carbohydrate Polymers*, 67(2):155–163.

Kaushik, A., Singh, M., Verma, G. (2010). Green nanocomposites based on thermoplastic starch and steam exploded cellulose nanofibrils from wheat straw. *Carbohydrate Polymers,* 82:337–345.

Krishnan, V.N., Ramesh, A. (2013). Synthesis and characterization of cellulose nanofibers from coconut coir fibers. *IOSR Journal of Applied Chemistry (IOSR-JAC),* 6(3):18–23.

Labeeuw, L., Martone, P.T., Boucher, Y., Case, R.J. (2015). Ancient origin of the biosynthesis of lignin precursors. *Biology Direct*, 10(1):1–21.

DOI: https//doi.org/10.22452/mjs.vol44no1.1
Malaysian Journal of Science 43(4): 1-8 (March 2025)

Lebo, S.E.J., Gargulak, J.D. and McNally, T.J. (2015). Lignin. *Kirk-Othmer Encyclopedia of Chemical Technology*. John Wiley & Sons, Inc. doi:10.1002/0471238961.12090714120914.a01.pub3

LeVan, S.L. (1989). Thermal degradation. In: Scniewind A.P. (Ed.), *Concise Encyclopedia of Wood and Wood-based Materials.* Pergamon Press, New York, 271–273.

Li, J. (2011). Isolation of Lignin from Wood. Saimaa University of Applied Sciences, Imatra Unit of Technology, Degree Programme in Paper Technology. Bachelor's Thesis, 2011.

Liu, D., Zhong, T., Chang, P.R., Li, K., Wu, Q. (2010). Starch composites reinforced by bamboo cellulosic crystals. *Biosource Technology,* 101:2529–2536.

Lu, Y., Sun, Q., She, X., Xia, Y., Liu, Y., Li, J., Yang, D. (2013). Fabrication and characterisation of α-chitin nanofibers and highly transparent chitin films by pulsed ultrasonication Carbohydrate Polymer, 98(2):1497–1504.

Martone, P.T., Estevez, J.M., Lu, F., Ruel, K., Denny, M.W., Somerville, C., Ralph, J. (2009). Discovery of lignin in seaweed reveals convergent evolution of cell-wall architecture. *Current biology, CB* 19(2):169–75.

Menon, M.P., Selvakumar, R., Ramakrishna, S. (2017). Extraction and modification of cellulose nanofibers derived from biomass for environmental application. *RSC Advances*, 7(68):42750–42773.

Ochigbo, S.S., Luyt, A.S., Mofokeng, J.P., Antic, Z., Dramicanin, M.D., Djokovic, V. (2012). Dynamic mechanical and thermal properties of the composites of thermoplastic starch and lanthanum hydroxide nanoparticles. *Journal of Applied Polymer Science,* doi:10.1002/APP.37859.

Okeniyi, J.O., Akinlabi, E.T., Akinlabi, S.A. and Okeniyi, E.T. (2019). Biochemical characterization data from Fourier transform infra-red spectroscopy analyses of *Rhizophora mangle* L. bark-extract. *Chemical Data Collections*, 19:100177.

Okeniyi, J.O., Popoola, A.P.I., Ojewumi, M.E., Okeniyi, E.T. and Ikotun, J.O. (2018). *Tectona grandis* capped silver-nanoparticle material effects on microbial strains inducing microbiologically influenced corrosion. *International Journal of Chemical Engineering*, 2018:7161537.

Okeniyi, J.O., John, G.S., Owoeye, T.F., Okeniyi, E.T., Akinlabu, D.K., Taiwo, O.S., Awotoye, O.A., Ige, O.J., Obafemi, Y.D. (2017a). Effects of *Dialium guineense* based zinc nanoparticle material on the inhibition of microbes inducing microbiologically influenced corrosion. In: Meyers, M.A., Benavides, H.A.C., Brühl, S.P., Colorado, H.A., Dalgaard, E., Elias, C.N., Figueiredo, R.B., Garcia-Rincon, O., Kawasaki, M., Langdon, T.G., Mangalaraja, R.V., Marroquin, M.C.G., da Cunha Rocha, A., Schoenung, J.M., Costa e Silva, A., Wells, M., Yang, W. *Proceedings of the 3rd Pan American Materials Congress*, Springer, Cham, 21–31.

Okeniyi, J.O., Omotosho, O.A., Inyang, M.A., Okeniyi, E.T., Nwaokorie, I.T., Adidi, E.A., Owoeye, T.F., Nwakudu, K.C., Akinlabu, D.K., Gabriel, O.O., Taiwo, O.S. (2017b). Investigating inhibition of microbes inducing microbiologically-influenced-corrosion by *Tectona grandis* based Fe-nanoparticle material. In: *AIP Conference Proceedings*, AIP Publishing LLC, 1814(1):020034.

Okeniyi, J.O. and Popoola, A.P.I. (2017). Understanding eco-friendly anticorrosion prospect on steel-reinforcement in NaCl-immersed concrete from biochemical characterization of *Irvingia gabonensis* leaf. *Contributed Papers from Materials Science and Technology 2017 (MS&T17)*, 1070–1077.

Okeniyi, J.O., Okeniyi, E.T., Ogunlana, O.O., Owoeye, T.F. and Ogunlana, O.E. (2016). Investigating biochemical constituents of *Cymbopogon citratus* leaf: Prospects on total corrosion of concrete steel-reinforcement in acidic-sulphate medium. In: *TMS 2017 146th Annual Meeting & Exhibition Supplemental Proceedings,* Springer, Cham, 341–351.

Paakko, M., Ankerfors, M., Kosonen, H., Nykanen, A., Ahola, S., Osterberg, M., Ruokolainen, J., Laine, J., Larsson, T., Ikkala, O. (2007). Enzymatic hydrolysis combined with mechanical shearing and high-pressure homogenization for nanoscale cellulose fibrils and strong gels. *Biomacromolecules*, 8(6):1934–1941.

Phanthong, P., Reubroycharoen, P., Hao, X., Xu, G., Abudula, A. and Guan, G. (2018). Nanocellulose: Extraction and application. *Carbon Resources Conversion*, 1(1):32–43.

Radotić K., Mićić M. (2016). "Methods for extraction and purification of lignin and cellulose from plant tissues." In: Mićić M. (eds) *Sample Preparation Techniques for Soil, Plant, and Animal Samples*. Springer Protocols Handbooks. Humana Press, New York, NY. doi:10.1007/978-1-4939-3185-9_26

Rahim, W.R.W.A., Idrus, R.M. (2018). Importance and uses of forest product bamboo and rattan: their value to socioeconomics of local communities. *International Journal of Academic Research in Business and Social Sciences*, 8(12):1484–1497.

Saito, T., Hirota, M., Tamura, N., Kimura, S., Fukuzumi, H., Heux, L., Isogai, A. (2009). Individualization of nano-sized cellulose fibrils by direct surface carboxylation using tempo catalyst under neutral conditions. *Biomacromolecules*, 10(7):1992–1996.

Salmén, L., Stevanic, J.S. and Olsson, A.M. (2016). Contribution of lignin to the strength properties in wood fibres studied by

DOI: https//doi.org/10.22452/mjs.vol44no1.1
Malaysian Journal of Science 43(4): 1-8 (March 2025)

dynamic FTIR spectroscopy and dynamic mechanical analysis (DMA). *Holzforschung*, 70(12):1155–1163.

Saniwan, S., Lalita, V. and Chularat, K. (2012). Starch/cellulose biocomposites prepared by high-shear homogenization/compression molding. *Journal of Materials Science and Engineering B,* 2(4):213–222.

Shahi, N., Min, B., Sapkota, B., Rangari, V.K. (2020). Eco-friendly cellulose nanofiber extraction from sugarcane bagasse and film fabrication. *Sustainability*, 12(15):6015.

Shi, Z.J., Xiao, L.P., Xu, F., Sun, R.C. (2012). Physicochemical characterization of lignin fractions sequentially isolated from bamboo (*Dendrocalamus brandisii*) with hot water and alkaline ethanol solution. *Journal of Applied Polymer Science*, 125(4):3290–3301.

Sumin, K., Lingping, X., Lingyan, M., Xueming, Z., Runcang, S. (2012). Isolation and structural characterization of lignin from cotton stalk treated in an ammonia hydrothermal system. *International Journal of Molecular Sciences,* 13:15209–15226.

Vazquez, A., Foresti, M.L., Cerrutti, P., Galvagno, M. (2013). Bacterial cellulose from simple and low cost production media by *Gluconacetobacter xylinus*. *Journal of Polymers and the Environment*, 21(2):545–554.

Visakh, P.M., Sabu, T. Kristiina O., Aji, P.M. (2012a). Crosslinked natural rubber nanocomposites reinforced with cellulose whiskers isolated from bamboo waste: Processing and mechanical/thermal properties. *Composites, Part A,* 43:735–741.

Visakh, P.M., Sabu, T., Kristiina, O., Aji, P.M. (2012b). Effect of cellulose nanofibers isolated from bamboo pulp residue on vulcanized natural rubber. *Bioresources,* 7(2):2156–2168.

Xiao, S., Gao, R., Lu, Y., Li, J., Sun, Q. (2015). Fabrication and characterization of nanofibrillated cellulose and its aerogels from natural pine needles. *Carbohydrate Polymers*, 119:202–209.

Yong, Z., Xiao-Bin, L., Chang, G., Wei-Jun, L., Ju-Ming, Y. (2012). Preparation and characterization of nano crystalline cellulose from bamboo fibers by controlled cellulase hydrolysis. *Journal of Fiber Bioengineering & Informatics*, 5(3):263–271.

Zakikhani, P. Zahari,R. Sultan, M.T.H., Majid, D.L. (2014). Bamboo fibre extraction and its reinforced polymer composite material. *International Journal of Chemical, Nuclear, Metallurgical and Materials Engineering*, 8(4):284–287.

Zhang, J., Elder, T.J., Pu, Y., Ragauskas, A.J., (2007). Facile synthesis of spherical cellulose nanoparticles. *Carbohydrate Polymers*, 69(3):607–611.

DOI: https//doi.org/10.22452/mjs.vol44no1.1
Malaysian Journal of Science 43(4): 1-8 (March 2025)